ChemTexts (2023) 9:5
https://doi.org/10.1007/s40828-022-00175-0

LECTURE TEXT

Molybdenum and tungsten: oxides, suboxides and oxide hydrates

Hans-Joachim Lunk[1] · **Hans Hartl**[2]

Received: 26 November 2022 / Accepted: 12 December 2022

Abstract

Synthesis, analysis, structure and applications of molybdenum and tungsten trioxides and dioxides as well as mixed-valence compounds have been described. The chapter *What is behind 'molybdic acid' and 'tungstic acid'?* explains and corrects the incorrect terms 'molybdic acid' and 'tungstic acid' for the hydrates $MoO_3 \cdot nH_2O$ ($n = 1, 2$) and $WO_3 \cdot nH_2O$ ($n = 1, 2, 0.5$). The chapter *Mixed molybdenum/tungsten trioxides* highlights the use of $Mo_nW_{1-n}O_3$ as antimicrobial substance.

Graphical Abstract

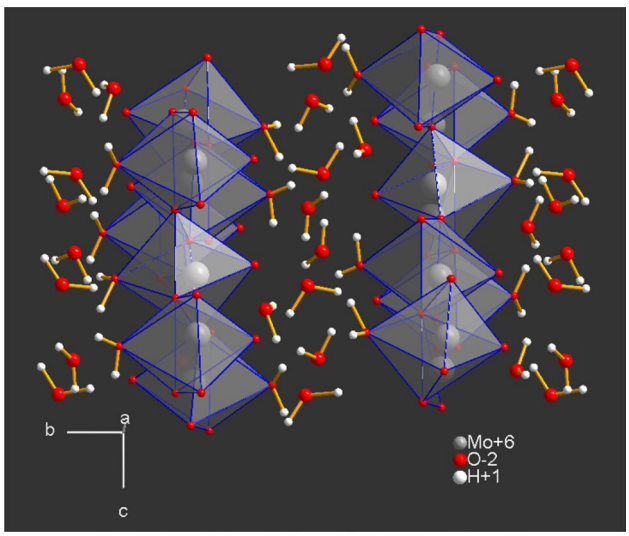

Keywords Molybdenum and tungsten oxides · Oxide hydrates · Applications · Mixed molybdenum/tungsten trioxides · Germ-free surfaces

Abbreviations

aka	Also known as
AMR	Antimicrobial resistance
b.p.	Boiling point
BET	Brunauer-Emmett-Teller
CS	Crystallographic shear
DOS	Density of states
HATB	Hexagonal ammonium tungsten bronze
K	Kelvin (0 K = − 273.15 °C)
kJ	Kilojoule (1 kJ = 0.2388 kcal)
kPa	Kilopascal (101.3 kPa = 1 atm)
LSPR	Localized surface plasmon resonance
MAS-NMR	Magic-angle spinning NMR
m.p.	Melting point

✉ Hans-Joachim Lunk
baaclunk@epix.net

Hans Hartl
hartl@zedat.fu-berlin.de

[1] Markkleeberg, Germany

[2] Institute of Chemistry and Biochemistry - Inorganic Chemistry, Freie Universität Berlin, Fabeckstr. 34/36, 14195 Berlin, Germany

Published online: 11 February 2023

NIRS	Near Infrared spectroscopy: From 12,820 cm^{-1} (780 nm) to 4000 cm^{-1} (2500 nm)
nm	Nanometer (1 nm = 10^{-9} m = 10^{-7} cm = 10 Å)
NMR	Nuclear magnetic resonance
ON	Oxidation number
PDF	Powder diffraction file
pm	Picometer (1 pm = 10^{-12} m = 10^{-10} cm = 0.01 Å)
ppm	Parts per million (1 ppm = 0.0001%)
POM	Polyoxometalate(s)
ρ (rho)	Symbol for density
SEM	Scanning electron microscopy
TBO	Tungsten blue oxide
XPS	X-ray photoelectron spectroscopy, aka ESCA (electron spectroscopy for chemical analysis)
XRD	X-ray diffraction
Z	Number of formula units in a unit cell

Basic properties of molybdenum and tungsten

Molybdenum: Group 6, Period 5 in the Periodic Table of Elements; Atomic number 42; Electron configuration $[Kr]4d^5 5s^1$; Molar mass 95.94 g mol^{-1}; m.p. 2623 °C

Tungsten: Group 6, Period 6 in the Periodic Table of Elements; Atomic number 74; Electron configuration $[Xe]4f^{14}5d^4 6s^2$ or $[Xe]4f^{14}5d^5 6s^1$; Molar mass 183.85 g mol^{-1}; m.p. 3420 °C

The metals molybdenum and tungsten belong to the 90 naturally occurring elements. As elements of the *d*-block in the Periodic Table, which includes groups 3–12, they are classified as 'transition elements' or 'transition metals.' Both metals also belong to the group of 'refractory metals.' These are a class of metals that are extraordinarily resistant to heat and wear. Most definitions of the term 'refractory metal' list the high melting point as a key requirement for inclusion. By one definition, a melting point above 2200 °C is necessary to qualify. The five elements niobium, molybdenum, tantalum, rhenium and tungsten are included in all definitions [1, 2].

Molybdenum oxides

Molybdenum trioxides

Molybdenum(VI) oxide, MoO_3, is formed during the roasting of many molybdenum compounds as a white solid at room temperature (ρ 4.69 g cm^{-3}; m.p. 795 °C; b.p. 1155 °C). According to mass spectrometric studies, the MoO_3 vapor (850 °C) contains mainly the polymeric species Mo_3O_9, Mo_4O_{12} and Mo_5O_{15} [3]. In contrast to tungsten trioxide, WO_3, molybdenum trioxide, MoO_3, reacts with acids as well as bases. Such substances are classified as *acid–base amphoteric compounds*,[1] aka *ampholytes*. The term is derived from the Greek word *ἀμφότερως* (amphoteros), meaning 'both.' When MoO_3 reacts with, e.g., HCl, it acts as a base to form the molybdenyl cation MoO_2^{2+}. When it reacts with, e.g., NaOH, it acts as an acid to form the monomolybdate anion, MoO_4^{2-}. Molybdenum trioxide forms five polymorphs. In addition to the thermodynamically stable α-MoO_3, four metastable polymorphs have been discovered.

Orthorhombic *α*-MoO_3

Orthorhombic α-MoO_3 (space group according to the *Hermann-Mauguin notation*[2]: *Pbnm*, $a = 1385.5$, $b = 369.6$, $c = 396.3$ pm) has a peculiar double-layer structure $^2_\infty MoO_{1/1}O_{2/2}O_{3/3}$ [4]. The layers are built up of MoO_6 octahedra at two levels, connected along the *b* axis by common edges and corners, to form zigzag rows, and along the *c* axis by common corners only (Fig. 1). Each MoO_6 octahedron has one double-bonded oxygen atom (Mo=O). Therefore, three kinds of structurally different oxygen atoms exist, namely terminal (singly coordinated), asymmetric bridging (twofold coordinated) and symmetric (threefold coordinated) bridging oxygen atoms.

Monoclinic *β*-MoO_3

Monoclinic β-MoO_3 was first synthesized by gently heated spray-dried molybdenum trioxide monohydrate, $MoO_3 \cdot H_2O$ (often incorrectly denominated 'molybdic acid', 'H_2MoO_4'), which had been prepared by passing sodium molybdate solution over an ion-exchange resin [5]. Powdered samples of β-MoO_3 have been obtained by gentle heat treatment of freeze-dried $MoO_3 \cdot H_2O$ at 350 °C for 1 h [6]. The XRD peaks were indexed on the basis of a monoclinic cell (space group $P2_1/c$). The cell parameters $a = 712.28$, $b = 533.6$, $c = 556.65$ pm and $\beta = 92.01°$ were determined. The structure of monoclinic β-MoO_3 is similar to monoclinic WO_3 and related to the three-dimensional ReO_3 structure, which consists of a corner-connected octahedral network, as shown in Fig. 2. An ab initio LAPW (linearized augmented planewave) study [7] of the α- and β-phases of bulk MoO_3 revealed that structure and electronic properties of α-MoO_3

[1] *Redox-amphoteric compounds* (aka *ampholytes*) are substances which react—depending on the reactant—as an oxidizing or reducing agent. H_2O_2 (oxidation number of oxygen −1) oxidizes, e.g., iodide, I^-, to I_2 and is reduced to H_2O (ON−2). On the other hand, it reduces, e.g., permanganate MnO_4^- to Mn^{2+} and is oxidized to O_2 (ON ± 0).

[2] *Hermann-Mauguin notation* is used to represent the symmetry elements in 32 crystallographic point groups and 230 space groups. It is named after the German crystallographer Carl Hermann (1888–1961), who introduced it in 1928, and the French mineralogist Charles-Victor Mauguin (1878–1958), who modified it in 1931. See also: International Tables for Crystallography: https://doi.org/10.1107/97809553602060000001

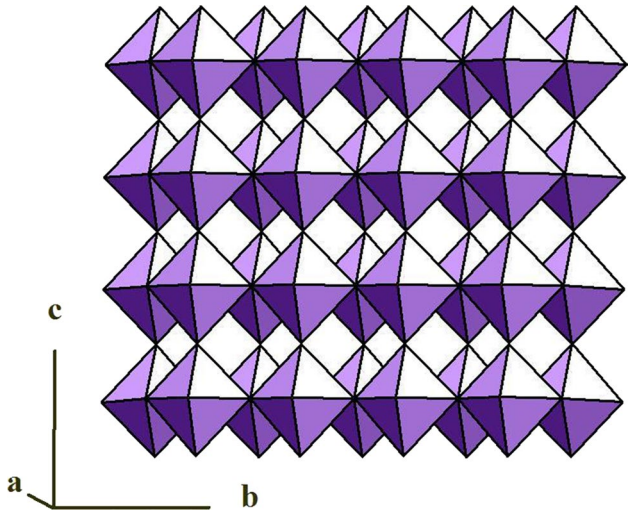

Fig. 1 Octahedral model of orthorhombic α-MoO_3

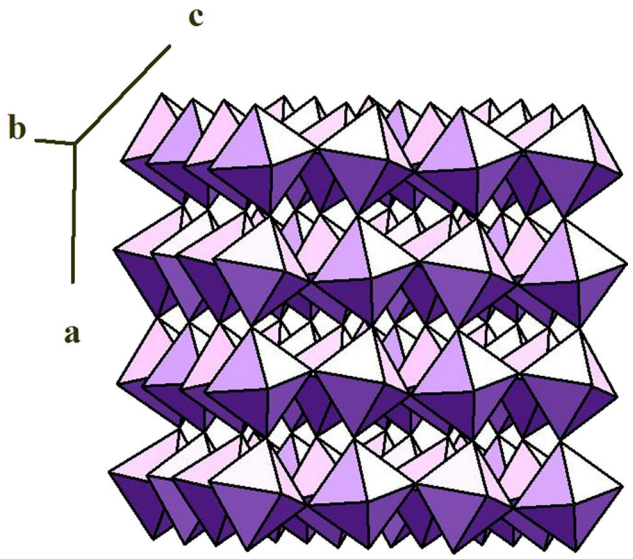

Fig. 2 Octahedral model of monoclinic β-MoO_3

are in good agreement with experimental and previous theoretical results. The orthorhombic modification is partially ionic, and the symmetrically bridging oxygen atoms exhibit more ionic character, while the terminal ones are more covalent. The characterization of the electronic structure of β-MoO_3 by density of states (DOS) disclosed that it is not a fully ionic system, containing certain covalent components. The $\beta \rightarrow \alpha$ transformation is both exothermic and photochromic. Above 400 °C at moderate heating rates, the yellow β-MoO_3 is converted to the white α-phase. The relatively high transformation temperature of β-MoO_3 is caused by its sufficient kinetic stability at room temperature. The partial substitution of molybdenum by tungsten stabilizes the ReO_3 structure (cf. chapter *Mixed molybdenum/tungsten trioxide for germ-free surfaces*).

Monoclinic β'-MoO_3

Another modification of molybdenum trioxide, designated β'-MoO_3, has been determined from neutron powder diffraction data and refined [8] using the *Rietveld refinement*.[3] At first, $D_{0.99}MoO_3$ was prepared by a *spillover reaction*.[4] β'-MoO_3 was produced by heating this intercalate in oxygen at 200 °C, driving off D_2O. The structure of β'-MoO_3 was refined as monoclinic ($P2_1/n$, $a = 742.45$, $b = 747.83$, $c = 768.97$ pm, $\beta = 90.09°$). It is isostructural with the room-temperature monoclinic modification of WO_3.

Monoclinic ε-MoO_3

The high-pressure modification ε-MoO_3 (or MoO_3-II) exhibits a specific monoclinic ($P2_1/m$) phase [9]. Similar to the α-MoO_3 structure, ε-MoO_3 has a layer structure. In fact, the individual $MoO_{1/1}O_{2/2}O_{3/3}$ layers of ε-MoO_3 and α-MoO_3 are virtually identical. However, the stacking sequence of the layers of ε-MoO_3 (*aaa*) differs from that of α-MoO_3 (*aba*), causing an improved packing efficiency for the layers of ε-MoO_3 versus those of α-MoO_3.

Hexagonal *h*-MoO_3

Finally, a vast variety of polymeric 'hexagonal molybdenum oxides' *h*-MoO_3 ($P6_3/m$ or $P6_3$) exists. Their structure can be best described by the formula $(NH_4)_x^3{}_\infty[Mo\square_{1-y}O_{3y}(OH)_x(H_2O)_{m-n}]\cdot nH_2O$ with $0.10 \le x \le 0.14$; $0.84 \le y \le 0.88$; $m + n \ge 3\text{-}x\text{-}3y$; $\square$ lattice vacancy. The hexagonal MoO_6 framework accommodates $[NH_4]^+$ cations, which float relatively freely in the structure's tunnels. The model of the phase *h*-MoO_3 is shown in Fig. 3 [10]. This phase, distinct among the other metastable MoO_3 polymorphs, allows a versatile intercalation chemistry with interesting chemical, electrochemical, electronic and catalytic properties [11].

[3] *Rietveld method* described by the Dutch crystallographer Hugo M. Rietveld (1932–2016) enables the structure refinement of non-monocrystalline powder samples.

See also: Young RA (1993) The Rietveld Method, Oxford University Press.

[4] *Spillover*, generally, is the transport of a species adsorbed or formed on a surface onto another surface.

In heterogeneous catalysis, hydrogen molecules can be adsorbed and dissociated by the metal catalyst.

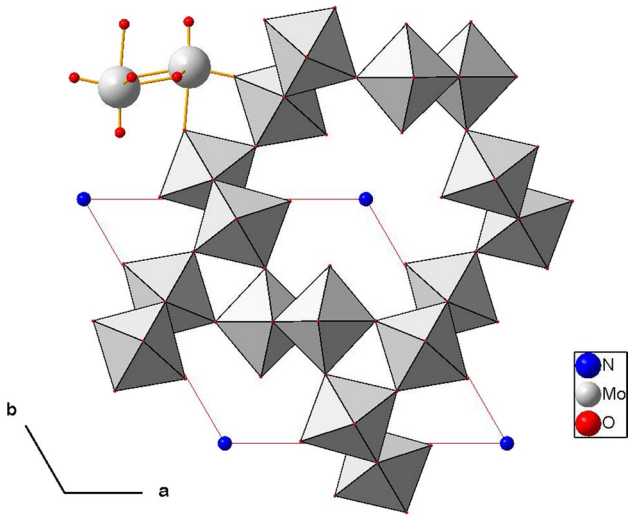

Fig. 3 Combined ball-and-stick/octahedral model of the *h*-MoO_3 framework (view along *c*-axis)

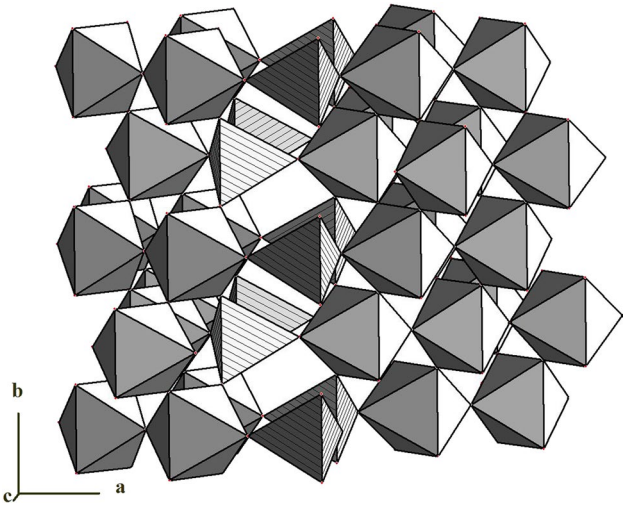

Fig. 4 Polyhedral model of the Magnéli phase γ-Mo_4O_{11}

Molybdenum dioxide

Brown-violet molybdenum(IV) oxide, MoO_2 (ρ 6.47 g cm^{-3}; m.p. 1100 °C), is formed by reduction of MoO_3 with hydrogen, ammonia, sulfur or carbon monoxide as well as electrolytically in molten salts. Above 1050 °C MoO_2 is noticeably volatile. Single crystals of MoO_2—as well as of WO_2—are available by chemical transport reactions [12]. The metallic conductor crystallizes in a distorted monoclinic rutile (TiO_2) structure. In TiO_2 the oxide anions are closely packed, and the titanium atoms occupy half of the octahedral interstices. In MoO_2 the Mo atoms are off-center, leading to alternating short and long Mo–Mo distances. The short Mo–Mo distance amounts to 251 pm, which is even less than the Mo–Mo distance of 272.5 pm in metallic molybdenum. The bond length is shorter than expected for a single bond. The bonding is complex and involves a delocalization of some of the Mo electrons in a conduction band accounting for the metallic conductivity [13].

Low-dimensional molybdenum oxides

A number of studies have been carried out on binary and ternary molybdenum oxides. These oxides are stable phases without extended homogeneity ranges. All structures of these oxides are composed of MoO_6 octahedra, MoO_4 tetrahedra and pentagonal MoO_7 bipyramids. These oxides of mixed valence belong to three structural classes: ReO_3, MoO_3 and a structure of a mixed-polygonal type [14].

A series of molybdenum oxides with a composition MoO_x ($2 < x < 3$) between MoO_3 and MoO_2 is formed, for example, when heating MoO_3 in vacuum or by reducing MoO_3 with Mo. The following phases exist: Mo_4O_{11} ($\triangleq MoO_{2.75}$), $Mo_{17}O_{47}$ ($\triangleq MoO_{2.765}$), Mo_5O_{14} ($\triangleq MoO_{2.80}$), Mo_8O_{23} ($\triangleq MoO_{2.875}$), $Mo_{26}O_{75}$ ($\triangleq MoO_{2.885}$), Mo_9O_{26} ($\triangleq MoO_{2.889}$) and $Mo_{13}O_{38}$ ($\triangleq MoO_{2.923}$). The phase diagram Mo–O has been established [15].

Low-dimensional compounds exhibit interesting physical properties associated with their electronic instabilities [16]. Red bronze $A_{0.33}MoO_3$ (A = Li, K, Rb, Cs, Tl) [17] is a semiconductor, while the phases Mo_4O_{11} [18, 19] as well as Mo_8O_{23} [20], blue bronze $A_{0.3}MoO_3$ (A = K, Rb, Tl) [21], purple bronze $A_{0.9}Mo_8O_{17}$ (A = Li, Na, K, Tl) [22], and the rare-earth bronze $La_2Mo_2O_7$ [23] exhibit metallic conductivity at room temperature. These phases are named *Magnéli phases* after the Swedish crystallographer Arne Magnéli (1914–1996). Structurally, all these oxides contain Mo–O layers made up of edge- and corner-sharing MoO_6 octahedra, with large and complex unit cells. The *Magnéli phase* Mo_4O_{11} exists in two modifications, γ- and η-Mo_4O_{11}. Both contain layers of Mo_6O_{22}, solely made up of MoO_6 octahedra. These layers are linked via MoO_4 tetrahedra to form the three-dimensional structures of γ-Mo_4O_{11} (Fig. 4). The γ- and η-phases differ slightly only in the way the Mo_6O_{22} layers are joined by the MoO_4 tetrahedra. The term 'crystallographic shear' to describe this type of structure was coined by Arthur David Wadsley (1918–1969) and elaborated by him in a seminal review of so-called non-stoichiometric compounds [24]. These solid inorganic compounds have compositions whose elemental proportions cannot be represented by integers. Contrary to Wadsley's definition of 'non-stoichiometric compounds' as 'mixtures of discrete chemical compounds,' the modern understanding views them as homogeneous. A small percentage of atoms is missing or too many atoms are packed into an otherwise perfect crystal lattice. Since the solids are overall electrically neutral, the

charge equalization is realized by either the same atoms with modified oxidation states or foreign elements with adequate charges. The guidelines for understanding the crystal structures as well as the chemical bonding and electronic properties of such complex systems are outlined in [25].

Tungsten oxides

The system tungsten-oxygen is very complex and structurally extremely adaptive. The important class of tungsten oxides is widely studied and used in many technological applications. While the fully oxidized phase, tungsten trioxide, has only corner-sharing WO_6 octahedra, a slight reduction results in edge-sharing between octahedra along crystallographic shear (CS) planes. Further reduction gives rise to formation of pentagonal column structures, in which at first the pentagonal columns are sharing corners only. With increased reduction, edge-sharing between the pentagonal columns is introduced [26].

Tungsten trioxide

Yellow tungsten(VI) oxide, WO_3 (ρ 7.16 g cm^{-3}; m.p. 1473 °C; b.p. ca. 1700 °C), is the ultimate oxidation product of all tungsten compounds. At about 1100 °C, WO_3 sublimates (sublimation heat 460 kJ mol^{-1}). The vapor contains the polymeric species W_4O_{12}, W_3O_9 and W_2O_6. When heating WO_3 in vacuum (1300–1500 °C) and during its reduction with tungsten powder in an inert atmosphere or with hydrogen, lower oxides WO_x ($2 < x < 3$) are formed. These are ordered phases with defined stoichiometry [27].

In contrast to the *acid–base amphoteric*[1] MoO_3, WO_3 reacts with bases only. It is characterized by a number of modifications originated from the ideal cubic perovskite-like structure under light distortion involving formation of WO_6 octahedra arranged in various corner- and edge-sharing configurations. Several temperature-dependent phase transitions occur. Thus, the monoclinic α-WO_3 phase exists below – 50 °C, followed by the triclinic β-WO_3 phase from − 50 to 17 °C and the monoclinic γ-WO_3 phase from 17 to 330 °C, which is stable at room temperature. The orthorhombic δ-WO_3 phase can be found at the temperature range of 330–740 °C. The tetragonal ε-WO_3 phase is detected above 740 ºC [28]. The high-temperature orthorhombic [29] and hexagonal h-WO_3 [30] phases have also been reported. In addition, the formation of metastable cubic WO_3 has been observed in the course of the dehydration of tungsten trioxide dihydrate, $WO_3 \cdot 2H_2O$ [31]. Tungsten oxides are attracting continuous attention as sensors to various gases, chromogenic (electro-, photo- and thermochromic) materials and catalysts in several acid-catalyzed or photocatalytic reactions. Hexagonal WO_3 can be prepared by annealing hexagonal ammonium tungsten bronze (cf. section *Tungsten bronzes).* Structure, composition and morphology of h-WO_3 were studied by XRD, XPS, Raman spectroscopy, ^{1}H-MAS-NMR, SEM and Brunauer-Emmett-Teller (BET) surface area measurement, while its thermal stability was investigated by in-situ XRD [32]. The octahedral representations of hexagonal h-WO_3 and monoclinic γ-WO_3 are shown in Figs. 5 and 6.

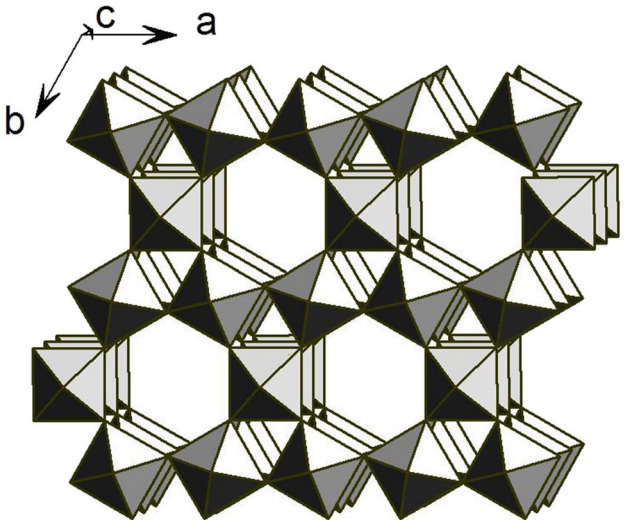

Fig. 5 Octahedral representation of hexagonal h-WO_3

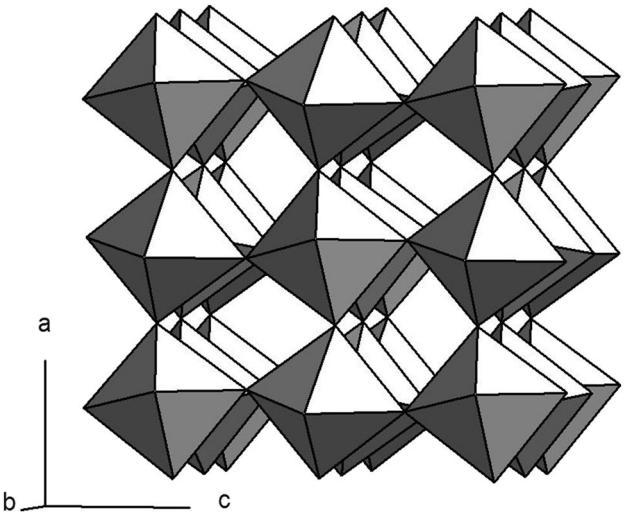

Fig. 6 Octahedral representation of monoclinic γ-WO_3

Tungsten dioxide

The chocolate brown tungsten(IV) oxide, WO_2 (ρ 10.8 g cm^{-3}; m.p. 1700 °C; b.p. 1730 °C), is an intermediate product of the reduction of tungsten compounds. It forms monoclinic crystals with a distorted rutile (TiO_2) structure and is therefore structurally very different from the higher

oxides. Each tungsten center has d^2 configuration, which gives the material a high-electric conductivity. WO_2 can be prepared by reduction of WO_3 with tungsten powder over the course of 40 h at 900 °C:

$$2WO_3 + W \rightarrow 3WO_2$$

The pure material is produced by reduction of WO_3 with moist hydrogen (e.g., at 900 °C, water vapor pressure 50 kPa) [33]. Single crystals are obtained by chemical transport technique using iodine. Because halides show oxidizing characteristics, tungsten oxyhalides are often formed as transport-effective species in which tungsten has a higher oxidation number than in the solid as shown for the transport of WO_2 with iodine [34]:

$$WO_2(s) + I_2(g) \rightleftarrows WO_2I_2(g)$$

Magnéli WO_n phases

In addition to five modifications of WO_3, several substoichiometric structures of WO_n, where n ranges from 2.625 to 2.92, have been experimentally observed. They are $W_{32}O_{84}$ ($\triangleq WO_{2.625}$), W_3O_8 ($\triangleq WO_{2.667}$), $W_{18}O_{49}$ ($\triangleq WO_{2.72}$), $W_{17}O_{47}$ ($\triangleq WO_{2.765}$), W_5O_{14} ($\triangleq WO_{2.80}$), $W_{20}O_{58}$ ($\triangleq WO_{2.90}$) and $W_{25}O_{73}$ ($\triangleq WO_{2.92}$). Their predominant preparation method is the heating of powder mixtures of WO_3 with tungsten or WO_2 in sealed, evacuated ampoules. Mineralizing and transporting agents, such as HCl and Cl_2, have sometimes been used to facilitate the reaction and improve the crystallinity of the suboxides formed. The crystal structures of *Magnéli phases* are found to be orthorhombic for $W_{32}O_{84}$ and W_3O_8, monoclinic for $W_{18}O_{49}$, $W_{17}O_{47}$, $W_{20}O_{58}$ and $W_{25}O_{73}$ and tetragonal for W_5O_{14}. These phases are characterized by formation of WO_7 pentagonal bipyramids surrounded by five edge-sharing WO_6 octahedra [26, 35]. The term 'crystallographic shear' to describe this type of structures was coined by Arthur David Wadsley (cf. section *Low-dimensional molybdenum oxides*).

Tungsten bronzes

By passing dry hydrogen over heated sodium tungstate, Na_2WO_4, the German chemist Friedrich Wöhler (1800–1882) observed in 1824 the formation of golden yellow crystals of metallic appearance. This was the first account of the formation of a tungsten bronze, a name originating from the metallic cluster characteristic of these compounds [36]. Tungsten bronzes are well-defined 'non-stoichiometric compounds' (cf. section *Magnéli phases*) of the general formula M_xWO_3 (M = H, Li, K, Rb, Cs, Fr, Be, Mg, Ca, Sr, Ba, Ra, Sc, Y, La, Ac, V, Nb; x is a variable < 1), most commonly with an alkali metal. For a considerable time, the tungsten bronzes were thought to be unique, but in recent years analogous compounds of molybdenum, vanadium, niobium and titanium have been prepared and found to have similar properties. The term 'bronze' is now applied to a ternary metal oxide of the general formula $M'_xM''_yO_z$ where M'' is a transition metal, M' is some other metal, and x is a variable falling in the range $0 < x < 1$. Such a compound possesses high electrical conductivity, is either metallic or semi-conducting, is intensely colored and shows metallic luster in crystalline form. It is chemically inert, and, through variation of x, sequences of solid phases occur, with definite and sometimes wide ranges of homogeneity [37].

Hexagonal ammonium tungsten bronze (HATB) is an important constituent of the intermediate tungsten blue oxide (TBO) in non-sag tungsten wire production [38]. Broad-line and high-resolution solid-state ^{1}H-NMR investigation of industrially manufactured TBOs and reference substances revealed a distinction between five proton-containing species. Henceforward, together with chemical, quantitative XRD and NH_4^+/K^+ ion-exchange analyses, a comprehensive characterization of different TBOs was available. Typically, TBO contains variable fractions of the crystalline compound HATB (cf. Fig. 5), monoclinic γ-WO_3 (cf. Fig. 6), tungsten suboxides like $W_{20}O_{58}$ and $W_{18}O_{49}$ as well as X-ray amorphous phases [39, 40].

Especially HATB, but also pyrochlore-related structures, are the basic structural motifs of many other metal oxides and metal fluorides, which are very promising heterogeneous catalysts in many different areas. As examples, two related publications are cited [41, 42].

What is behind 'molybdic acid' and 'tungstic acid'?

In the system MoO_3–H_2O two compounds of the formal composition $MoO_3 \cdot H_2O$ and $MoO_3 \cdot 2H_2O$ exist. The system WO_3–H_2O is characterized by the hydrates $WO_3 \cdot H_2O$, $WO_3 \cdot 2H_2O$ and $WO_3 \cdot 0.5H_2O$. Broadline ^{1}H-NMR and IR/Raman spectroscopic studies as well as X-ray single-crystal structure studies have shown that water in all five hydrates is present in the form of H_2O. Molecular species akin to sulfuric acid, H_2SO_4, i.e., 'H_2MoO_4' and 'H_2WO_4,' do not exist. The denominations 'molybdic acid' and 'tungstic acid,' still applied in numerous scientific publications and sale advertisements for these compounds, are definitely incorrect and should not be used in a chemical description.

'Molybdic acid'

Molybdenum trioxide dihydrate, $MoO_3 \cdot 2H_2O$, crystallizes as yellow crystals when a solution of ammonium paramolybdate, $(NH_4)_6[Mo_7O_{24}] \cdot 4H_2O$, in fairly concentrated nitric acid is stored for a long time. The sample of the composition $MoO_3 \cdot 1.1H_2O$ was prepared by slow dehydration of

the dihydrate at room temperature in a vacuum desiccator. More than 60 years ago, proton magnetic resonance experiments were carried out in an attempt to answer the question 'hydrate' or 'acid?' [43]. At 77 K, the second moments of the absorption curves amounted to 30.7 ± 1.6 gauss^2 for $MoO_3 \cdot 2H_2O$ and 27.6 ± 1.4 gauss^2 for $MoO_3 \cdot 1.1H_2O$. Line shapes were recorded for samples ranging from $MoO_3 \cdot 2H_2O$ to $MoO_3 \cdot 1.1H_2O$ at temperatures of 77 K and 290 K.

The Infrared spectra of the two hydrates, compared to those of MoO_3, provided additional evidence. The samples showed broad Infrared absorption bands with maxima at the following frequencies (cm^{-1}; *m* medium, *w* weak, *sh* shoulder) $\underline{MoO_3 \cdot 2H_2O}$: 3100 m, 2336 w, 1592 m, 963 m, 909 m; $\underline{MoO_3 \cdot 1.1H_2O}$: 2,326 w, 1,140 sh, 1081 sh, 980 m, 823 w; $\underline{MoO_3}$: 3200 m, 2326 w, 1600 m, 1122 sh, 926 m. The pairs of frequencies 3100/1592 and 3200/1600 cm^{-1} are absent from the spectrum of MoO_3 and are therefore attributed to water frequencies characteristic of the hydrated crystals. The lines at 1592 and 1600 cm^{-1} in the dihydrate and monohydrate are attributed to an O–H bending frequency and are little changed from the value of 1600 cm^{-1} in water vapor. The maxima at 3100 and 3200 cm^{-1} are attributed to the stretching frequencies and are considerably removed from the values in water vapor of 3652 and 3756 cm^{-1}. Such shifts are well known to occur in hydrogen-bonded compounds, and there is a general tendency for the O–H stretching frequency to decrease with a shortening of the O–H···O distance. The nuclear magnetic resonance results gave only the inter-proton distance (156 ± 3 pm) in the water molecule; the O–H distance is not derived until the HOH angle is known. Assuming that this angle is the same as that in water vapor (104° 28'), the proton magnetic resonance results give an O–H distance of 99 pm, which is very close to the value of 98 pm suggested by the data assembled in [44].

The Raman and Infrared spectra of $MoO_3 \cdot 2H_2O$ and $MoO_2Cl_2 \cdot H_2O$ have been assigned based on the known crystal structures of these compounds. In the region of the Mo–O stretching frequencies, the spectra of $MoO_3 \cdot 2H_2O$ and MoO_2C1_2 or WO_2C1_2 are very similar. The same is valid for $MoO_3 \cdot 2H_2O$ compared with MoO_3. The frequency ν_{as}(Mo–O–Mo) depends highly on the ratio of the bond lengths of the two bridge bonds [45].

Single crystals of the white molybdenum trioxide monohydrate, $MoO_3 \cdot H_2O$, were transformed by heating to 160 °C into perfect pseudomorphs built up from oriented MoO_3 crystallites of known structure. From the mutual orientation relationship of the unit cells of both phases involved in this *topotactic reaction*,[5] as determined by X-ray photographs, a model for the so far unknown crystal structure of white $MoO_3 \cdot H_2O$ could be deduced. Independently, the structure of $MoO_3 \cdot H_2O$ was determined by X-ray diffractometer data: Triclinic space group $P1$: $a = 738.8$, $b = 370.0$, $c = 667.3$ pm; $\alpha = 107.8$, $\beta = 113.6$, $\gamma = 91.2°$; $Z = 2$. The structure is built up from isolated double chains of strongly distorted $[MoO_5(H_2O)]$ octahedra sharing two common edges with each other. This result agrees well with the model derived from *topotaxy* (see Footnote 5), and it becomes evident how the MoO_3 lattice is formed through corner linking of the isolated double chains after the water molecules are removed. The study of topotactic phenomena seems rather generally applicable to deduce the main features of structures involved and for better understanding of structural relationships. The monohydrate consists of layers of octahedrally coordinated $MoO_5(H_2O)$ units where four vertices are shared [46].

The crystal structure of molybdenum trioxide dihydrate, $MoO_3 \cdot 2H_2O$, has been determined based on three-dimensional X-ray diffractometer data [47]. It crystallizes in the monoclinic space group $P2_1/n$ in a superstructure unit cell of dimensions $a = 1047.6(5)$, $b = 1382.2(6)$, $c = 1060.6(5)$ pm, $\beta = 91.62(3)°$; $Z = 16$. The structure consists of a system of infinite $[MoO_3(H_2O)]_n$ layers. Five oxygen atoms and one H_2O molecule form a strongly distorted octahedron around Mo. Every octahedron shares a corner with each of four neighboring octahedra within the layers. The octahedra form characteristic zigzag rows within the layers, with alternating short (176.6/180.0 pm) and long (215.6/205.4 pm) Mo–O bridge bond distances. The bonded hydrate molecule was identified by the long axial Mo–O distance of 228.8 pm, as opposed to the short axial (terminal) Mo–O bond of 169.4 pm (Fig. 7), by analogy to the structure of $WO_3 \cdot H_2O$ (Fig. 8). The second half of the water molecules is not bonded to Mo, but acts as hydrate water in the voids between the layers, each inter-layer H_2O molecule being in hydrogen-bonding contact with both neighboring layers. The compound should therefore be correctly referred to as molybdenum hydrato-trioxide hydrate, $[MoO_{4/2}O(OH_2)] \cdot H_2O$ or molybdenum-aquo-trioxide hydrate, $[MoO_3(OH_2)] \cdot H_2O$. $MoO_3 \cdot 2H_2O$ was the first example of an oxide hydrate with both coordinated and hydrate water molecules.

[5] A *topotactic reaction* (*topotaxy*) is a chemical solid-state reaction such that the orientations of the product crystals are determined by the orientation of the initial crystal.

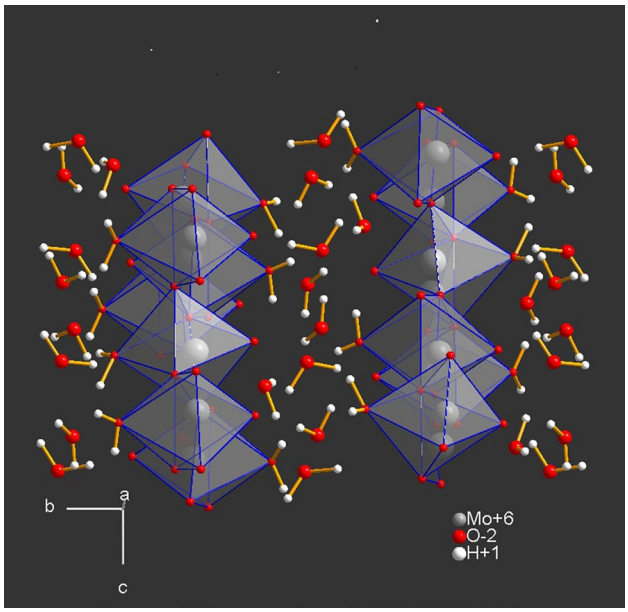

Fig. 7 Combined ball-and-stick/octahedral model of the $MoO_3{\cdot}2H_2O$ framework

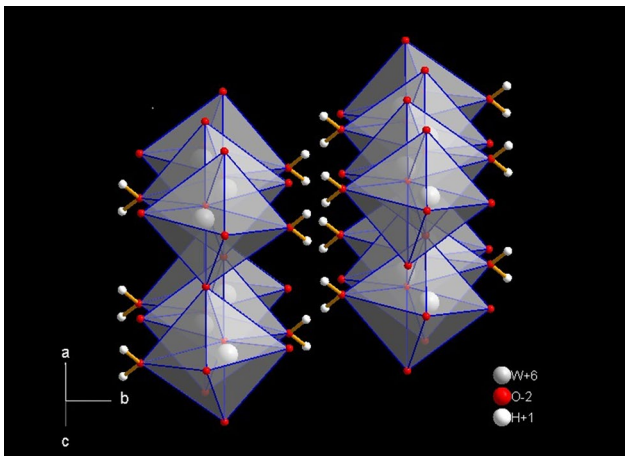

Fig. 8 Combined ball-and-stick/octahedral model of the mineral *tungstite*, $WO_3{\cdot}H_2O$

'Tungstic acid'

The term 'tungstic acid' incorrectly refers to tungsten trioxide monohydrate, $WO_3{\cdot}H_2O$ {ρ 5.59 g cm^{-3}; m.p. 100 °C (decomposes); b.p. 1473 °C}, tungsten trioxide dihydrate, $WO_3{\cdot}2H_2O$, and tungsten trioxide hemihydrate, $WO_3{\cdot}0.5H_2O$. The dihydrate forms as a precipitate of strongly acidified aqueous tungstate solutions at 25 °C and is transformed into the monohydrate at 50–100 °C. IR spectra and ^{1}H-NMR results have shown that tungsten trioxide di- and monohydrate contain the water as crystal water [48].

The X-ray single-crystal study of the mineral *tungstite*, $WO_3{\cdot}H_2O$ [49], confirmed the spectroscopic findings [48] for $WO_3{\cdot}H_2O$. *Tungstite* is a mineral, formed as an oxidation product of the minerals *wolframite*, (Fe, Mn)WO_4, *scheelite*, $CaWO_4$, and other *primary tungsten minerals*.[6] It was not possible to isolate enough pure material of *tungstite* for a microprobe analysis or for a bulk analysis of $WO_3{\cdot}H_2O$. However, the powder-diffraction data of *tungstite* fit synthetic $WO_3{\cdot}H_2O$ (PDF 18-1418). The crystal structure of *tungstite* has been solved from single-crystal X-ray-diffractometer data collected with MoKα radiation and has been refined to an *R factor*[7] of 4.3%. *Tungstite* is orthorhombic, *Pmnb* with $a = 524.9$, $b = 1071.1$, $c = 513.3$ pm; $Z = 4$. Its layer-like structure (Fig. 8) illustrates the interlayer hydrogen bonding. Each tungsten atom is octahedrally coordinated by five oxygen atoms and one water molecule. The W–O bond lengths of the four twofold coordinated oxygen atoms amount to 183.3 pm (2x) and 193.3 pm (2x). The water molecule is identified by the long axial bond of 233.9 pm, as opposed to the short axial (terminal) W–O bond of 168.8 pm, by analogy to the structure of $MoO_3{\cdot}2H_2O$ (Fig. 7). The sheets are held together by a network of hydrogen bonds, such that the water axial position in a given octahedron bonds two axial atoms from octahedra in the adjacent layer. Thus, a zigzag pattern of hydrogen bonds is formed, extending in the *c* direction, as illustrated in Fig. 8.

Cubic *pyrochlore-type*[8] $WO_3{\cdot}0.5H_2O$ has been synthesized hydrothermally directly from a solution of Na_2WO_4 and HCl in closed tubes at 155 °C. Its crystal structure has been determined by X-ray diffraction of a single crystal: Space group *Fd*3*m*, $a = 1030.5(3)$ pm; $Z = 16$. The structure contains corner-sharing WO_6 octahedra, leaving tunnels along the direction [110], in which the water molecules are located [50]. $WO_3{\cdot}0.5H_2O$ is representative of defect pyrochlores. The structure of oxide pyrochlores, with the general formula $A_2B_2O_6O'$, tolerates chemical substitution at the A, B, O and O' sites as well as vacancies at the A and O' sites. In $WO_3{\cdot}0.5H_2O$ ($W_2O_6{\cdot}H_2O$), the sites of the A-cations are unoccupied and the crystal water is located at the O' sites.

[6] A *primary mineral* or *magmatic rock* is any mineral formed during the original crystallization of the host igneous rock (derived from the Latin word *ignis* meaning *fire*). *Igneous rock* is formed through the cooling and solidification of magma or lava.

[7] In crystallography, the *R factor* is a measure of the agreement between the crystallographic model and the experimental X-ray diffraction data. In other words, it is a measure of how well the refined structure predicts the observed data.

[8] The *pyrochlore group* gets its name from the generic name *pyrochlore*, which was first introduced by Jöns Jakob Berzelius (1779−1848) for a cubic mineral found by Nils Otto Tank (1800−1864) in the 1820s in a syenite pegmatite at Stavern (formerly Fredriksvärn), Norway. The name is derived from the Greek *πῦρ* (fire) and *χλωρός* (green) in allusion to the fact that the mineral usually turns green on ignition.

Applications of molybdenum oxides

Molybdenum(VI) oxide, MoO_3, is produced on the largest scale of any molybdenum compound. Its primary application is as an oxidation catalyst and as a raw material for the production of molybdenum metal. Orthorhombic α-MoO_3 is a wide-bandgap *n*-type semiconductor, which is very attractive for different technological applications such as photochromic materials, smart windows, self-developing photography, conductive gas sensors, lubricants and catalysts [51]. Hexagonal molybdenum trioxide, *h*-MoO_3, has the potential application for secondary lithium-ion batteries [52] when it is obtained as well-faceted rods [53]. It also presents photoluminescent properties with emission bands at 436, 606 and 668 nm when excited at 330 nm [54].

Molybdenum trioxide, a cathodically blue coloring substance, is known as an electrochromic compound nearly as long as tungsten trioxide. Its properties and behavior resemble that of WO_3 in many aspects (cf. section *Applications of tungsten oxides*).

A recent study investigated the cytotoxicity of molybdenum trioxide nanoplates toward invasive breast cancer cells by analyzing morphological changes and performing the corresponding analyses. The findings suggested that MoO_3 exposure induces *apoptosis* (programmed cell death) and generates reactive oxygen species in these cells. The study revealed the potential utility of MoO_3 for treating metastatic cancer cells, which might enable advancements in cancer therapy [55].

Applications of tungsten oxides

Tungsten oxides are attracting continuous attention as sensors to various gases, chromogenic (electro-, photo- and thermochromic) materials and catalysts in several acid-catalyzed or photocatalytic reactions. From the beginning of *electrochromics*[9] research in the 1960s until today, tungsten trioxide is by far the most popular electrochromic material, which has been investigated intensively. Thin layers of the yellow compound WO_3, with a thickness < 1000 nm, are largely uncolored. Such a thin film can be reduced by electrochemical means to a deep-blue reduced form of tungsten trioxide. Therefore, tungsten trioxide is a cathodic electrochromic compound. During this reduction, charge balancing cations (M^+) such as H^+, Li^+ or K^+ are intercalated in the tungsten oxide structure. By electrochemical oxidation, this process can be reversed: $\overset{\text{blue}}{M_xWO_3} \rightleftarrows \overset{\text{uncolored}}{WO_3} + xe^- + xM^+ (x \leq 0.3)$ [56].

The recently published review article [57] summarizes the comprehensive progress made in the last few years in the application of tungsten oxide-based materials, WO_{3-x}, M_xWO_3 and their hybrid materials, as interesting research topics, particularly for morphology control and composite construction to enhance optical absorption, charge separation, redox capability and electrical conductivity. The solvothermal treatment is the most used method alongside the hydrothermal treatment, which is a facile and cost-effective method that can produce WO_x with different nanomorphologies. The morphology can be fine-tuned by controlling variables such as time, precursor concentration and temperature. A critical challenge is to enhance the utilization efficiency by extending the solar spectrum response from the UV to the NIR region. To meet these requirements, hybrids of $WO_{2.72}$ and M_xWO_3 have become important because of their strong photo-absorption ability and intervalence charge properties. A major advantage of this material is the 'localized surface plasmon resonance' (LSPR) effect, which may encourage researchers to focus not only on the interesting properties for new applications but also to investigate the many opportunities it offers to improve the efficiency of current applications.

Mixed molybdenum/tungsten trioxides

Resistance to antibiotics

The worldwide increase of multi-resistant microorganisms is responsible for millions of deaths per year [58]; 4.95 million deaths according to a recent study were linked to an antibiotic-resistant bacterial infection in 2021; 1.27 million people died directly from infection with a resistant bacterium. Without resistance, these deaths would have been preventable [59]. In the *Report on Antibiotic Resistance*, bacterial resistance was seen as one of the most common cause of death worldwide and requires immediate, innovative and ambitious action [60–62]. Much emphasis is therefore based on the prevention of *nosocomial infections*[10] with multi-resistant microorganisms. The crucial initial step however is the investigation of the reasons for development of 'multi drug-resistant' (MDR) microorganisms.

Viral infections of the upper respiratory tract are frequently observed in children and predisposed patients for bacterial superinfections, e.g., *sinusitis* (inflammation of

[9] *Electrochromic materials* are able to vary their coloration and transparency to solar radiation, in a reversible manner, when they are subjected to a small electric field (1–5 V). Important materials with electrochromic properties are oxides of transition metals, in particular WO_3, MoO_3, IrO_2, NiO and V_2O_5.

[10] *Nosocomial infections*, also referred to as *healthcare-associated infections* (HAI), are infections acquired during the process of receiving health care that was not present during the time of admission.

the paranasal sinuses), *otitis media* (inflammatory diseases of the middle ear) or bronchitis, and rarely pneumonia or bloodstream infections, where the administration of antibiotics is mandatory [63, 64]. Antibiotics have to be administered only once a bacterial superinfection has been documented. This requires frequent clinical controls of the patient. Prophylactic antibiotics are not helpful for the prevention of these bacterial superinfections. Prophylaxis of bacterial superinfections is feasible with an approach other than antibiotics. Effective alternatives are, e.g., anti-inflammatory properties based on herbal extracts (thyme, gentian, primula) which open clogged paranasal sinus openings as well as the patency of the Eustachian tube and improve the 'mucociliary clearance' (MCC) [65]. These herbal extracts have been used for > 70 years to treat patients who have infectious diseases.

Since the 1940s, antimicrobial agents have greatly reduced illness and death from these diseases. However, the drugs have been used so widely and for so long that the infectious organisms the antibiotics are designed to kill have adapted to them, making the drugs less effective. 'Antimicrobial resistance' (AMR) threatens the effective prevention and treatment of an ever-increasing range of infections caused by bacteria, parasites, viruses and fungi. AMR is an increasingly serious threat to global public health. It occurs naturally over time, usually through genetic changes. However, the misuse and overuse of antimicrobials accelerate this process.

Antimicrobial surfaces

There is a strong and growing need for antimicrobial surfaces. Most antimicrobials today work well in a laboratory environment, where efficacy tests with bacteria are made according to standards. However, these tests normally do not take into account the duration of antimicrobial activity in 'real-world' settings where 'shielding' of the antimicrobial agent by low ambient humidity, rapid elution (washing out) by water/disinfectants or the inactivation by sulfur-containing compounds can—and do—occur. In the healthcare sector, the formation of resistances and allergies is another topic of serious concern with antimicrobials. The following precautions and procedures are effective only in a limited way and are generally very costly.

- The 'Dutch model': admission of each patient into an isolation ward to investigate his or her colonization with resistant microorganisms.
- Personnel-intensive care: the one-to-one nursing care to an individual patient for a period of time results in a 70% reduction of hospital-acquired infections.
- Impregnation of biomaterials with disinfectants: limited spectrum of activity and toxicity. Disinfectants annihilate the entire flora and destabilize the skin.
- Extensive hand washing: healthcare workers' hands are the most common vehicle for the transmission of healthcare-associated pathogens from patient to patient and within the healthcare environment.
- The activity of silver/copper technologies is limited to 7−90 days.
- Application of organic biocides like formaldehyde, HCHO, and phosphorus-, sulfur- or halogen-containing polymers.

Many antimicrobial products that contain silver, copper or organic biocides fall short of their expectations. There is a need for antimicrobial surfaces in critical areas, such as hospitals, foster homes, airports, trains, public spots and the food processing industry, to prevent the spread of multi-resistant pathogenic microorganisms and viral infections.

In situ-generated biocides by catalysts like molybdenum trioxide, MoO_3, tungsten blue oxide (cf. section *Hexagonal ammonium tungsten bronze*), zinc molybdate, $ZnMoO_4$, and POMs (polyoxometalates) [66] show fast antimicrobial activity against a very broad spectrum of bacterial pathogens.

Molybdenum/tungsten trioxides create germ-free surfaces

It was shown that molybdenum trioxide, MoO_3, and tungsten trioxide, WO_3, provide antimicrobial activity, when dispersed in various polymers. By catalyzing the formation of oxonium, H_3O^+, on the surface of the materials, they mimic natural defense mechanisms of the human skin [67].

The water solubility of MoO_3 (1.4 g L^{-1} at 25 °C) excludes the use of pure MoO_3-based antimicrobial surfaces from application, where a constant contact with water and a long lifetime are required. The use of mixed Mo/W trioxides obviates the water solubility of MoO_3. The solid solutions $Mo_nW_{1-n}O_3$ combine the higher antimicrobial activity of MoO_3 with the virtual insolubility of WO_3 in water. Therefore, the successful testing of solid solutions $Mo_nW_{1-n}O_3$ ($0 < n < 1$) revealed a significant improvement of the MoO_3 method [68].

Synthesis of $Mo_nW_{1-n}O_3$

Monocrystals of $Mo_nW_{1-n}O_3$ were first grown by heating ground mixtures of MoO_3 and WO_3. The mixtures were pressed to pellets, sealed in quartz tubes and heated up to 1100 °C for 3 days. The structures of 12 identified phases were closely related to the corresponding monoclinic WO_3 phase (Fig. 6) except for $n > 0.95$, where an orthorhombic

MoO_3-like structure was found [69]. Since then, six alternative preparation methods were described:

- Precipitations of ammonium molybdotungstate from aqueous solutions of ammonium paratungstate, $(NH_4)_{10}[H_2W_{12}O_{42}]\cdot 4H_2O$, and ammonium paramolybdate, $(NH_4)_6[Mo_7O_{24}]\cdot 4H_2O$ [70, 71].
- Co-crystallization of mixed ammonium molybdotungstates by evaporation in a fan oven at 110 °C followed by calcination at 500 °C [72].
- The mixed hydrates $Mo_nW_{1-n}O_3\cdot H_2O$ were prepared by dissolving corresponding amounts of MoO_3 and WO_3 in a minimum quantity of ammonia and then adding the obtained solution dropwise to hot 6 M nitric acid under constant stirring. The dehydration of the mixed hydrates resulted in $Mo_nW_{1-n}O_3$ having the ReO_3− like structure [73].
- Dehydration of the hydrated mixed oxides $Mo_nW_{1-n}O_3\cdot 1/3H_2O$, prepared by the *chimie douce method*,[11] at about 300 °C [74].
- Spray-drying an aqueous solution, which contains a mixture of $MoO_3\cdot nH_2O$ and $WO_3\cdot nH_2O$ ($n=1$, 2; cf. chapter *What is behind 'molybdic acid' and 'tungstic acid'?*).

The starting aqueous solutions were prepared by cation exchange method from sodium molybdate, Na_2MoO_4, and sodium tungstate, Na_2WO_4. The spray-dried precursors were heated at 300 °C in oxygen [75]. A contamination of the solid solution with about 200 ppm Na was detected.

- Freeze-drying an aqueous solution of $MoO_3\cdot nH_2O$ and $WO_3\cdot nH_2O$ and heating the resulting powder to temperatures between 275 and 325 °C [76]. As in the previous preparation method, a contamination of the final product with sodium was observed.

The new and convenient method for synthesizing solid solutions $Mo_nW_{1-n}O_3$ guarantees a sodium-free product [68]. Spray drying of aqueous solutions of ammonium dimolybdate, $(NH_4)_2Mo_2O_7$, and ammonium metatungstate, $(NH_4)_6[H_2W_{12}O_{40}]\cdot 3H_2O$, resulted in precursors which were subsequently calcined at 300−600 °C. The obtained yellowish powders were ground and characterized by chemical analysis and XRD. After calcination at ≥ 400 °C only traces of H_2O and NH_3 were detectable. The materials were dispersed in concentrations of up to 2% into the polymers polypropylene (PP), polyethylene (PE), polyvinylchloride (PVC) and thermoplastic polyurethane (TPU). The antimicrobial effect was determined using the so-called drop-on as well as the roll-on method in concentrations of 10^6−10^9 CFU mL^{-1} (colony-forming units per milliliter) against the reference germs 'methicillin-resistant *Staphylococcus aureus*' (MRSA, S.a.), '*Escherichia coli*' (*E. coli*, E.c.) and '*Pseudomonas aeruginosa*' (*P. aeruginosa*, P.a.). The solid solutions $Mo_{0.25}W_{0.75}O_3$ and $Mo_{0.75}W_{0.25}O_3$ delivered the best results (Fig. 9).

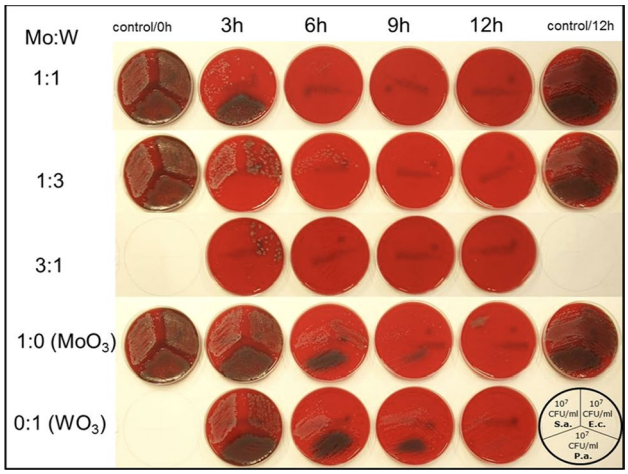

Fig. 9 Antimicrobial tests of $Mo_nW_{1-n}O_3$, MoO_3 and WO_3 (2% oxide in thermoplastic urethane): Drop-on method with the three reference germs S.a., E.c. and P.a. (10^7 CFU mL^{-1})

Author contributions H-JL wrote the main manuscript text. HH created the figures. Both authors reviewed the manuscript.

Data availability No data was used for the research described in the article.

Declarations

Conflict of interest The authors declare no competing interests.

References

1. Lunk HJ, Hartl H (2017) Discovery, properties and applications of molybdenum and its compounds. ChemTexts 3:13. https://doi.org/10.1007/s40828-017-0048-6
2. Lunk HJ, Hartl H (2019) Discovery, properties and applications of tungsten and its inorganic compounds. ChemTexts 5:15. https://doi.org/10.1007/s40828-019-0088-1
3. Berkowitz J, lnghram MG, Chupka WA (1957) Polymeric gaseous species in the sublimation of molybdenum trioxide. J Chem Phys 26:842–845
4. Kihlborg L (1963) Least squares refinement of the crystal structure of molybdenum trioxide. Arkiv Kemi 21:357–364
5. McCarron EM III (1986) β-MoO_3: a metastable analogue of WO_3. J Chem Soc Chem Commun 1986:336–338
6. Parise JB, McCarron EM III, Von Dreele R, Goldstone JA (1991) β-MoO_3 produced from a novel freeze drying route. J Solid State Chem 93:193–201
7. Sayede AD, Amriou T, Pernisek M, Khelifa B, Mathieu C (2005) An ab initio LAPW study of the [alpha] and [beta] phases of bulk molybdenum trioxide, MoO_3. Chem Phys 316:72–82
8. Parise JB, McCarron EM III, Sleight AW (1987) A new modification of ReO_3-type MoO_3 and the deuterated intercalation

[11] *Chimie douce* (soft chemistry) is a technique that uses reactions at moderate temperature in open reaction vessels under conditions similar to those in biological systems.

compound from which it is derived: $D_{0.99}MoO_3$. Mater Res Bull 22:803–811
9. McCarron EM III, Calabrese JC (1991) The growth and single crystal structure of a high pressure phase of molybdenum trioxide: MoO_3-II. J Solid State Chem 91:121–125
10. Lunk HJ, Hartl H, Hartl MA, Fait MJG, Shenderovich IG, Feist M, Frisk TA, Daemen LL, Mauder D, Eckelt R, Gurinov AA (2010) "Hexagonal molybdenum trioxide"—known for 100 years and still a fount of new discoveries. Inorg Chem 49:9400–9408
11. Guo J, Zavalij P, Whittingham MS (1994) Preparation and characterization of a MoO_3 with hexagonal structure. Eur J Solid State Inorg Chem 31:833–842
12. Schäfer H, Grofe T, Trenkel M (1973) The chemical transport of molybdenum and tungsten and of their dioxides and sulfides. J Solid State Chem 8:14–28
13. McCarroll WH, Ramanujachary (2011) Oxides: solid-state chemistry. https://doi.org/10.1002/9781119951438.eibc0161
14. Robin M, Day P (1968) Mixed-valence chemistry: a survey and classification. Adv Inorg Chem Radiochem 10:247–422
15. Chang LLY, Phillips B (1969) Phase relations in refractory metal-oxygen systems. J Am Ceram Soc: 527–533
16. Greenblatt M (1988) Molybdenum oxide bronzes with quasi-low-dimensional properties. Chem Rev 88:31–53
17. Canadell E, Whangbo MH (1988) Semiconducting properties of lithium molybdate, $Li_{0.33}$ MoO_3. Inorg Chem 27:228–232
18. Magnéli A (1948) The crystal structure of Mo_4O_{11} (γ-molybdenum oxide). Acta Chem Scand 2:861–871
19. Schlenker C, Dumas J, Escribe-Filippini C, Guyot H, Marcus J, Fourcaudot C (1985) Charge-density-wave instabilities in the low-dimensional molybdenum bronzes and oxides. Philos Mag 52B:643–667
20. Sato M, Fujishita H, Sato S, Hoshino S (1986) Structural transitions in Mo_8O_{23}. J Phys C 19:3059–3067
21. Ganne M, Boumaza A, Dion M, Dumas J (1985) The blue bronze $Tl_{0.30}MoO_3$ structure and physical properties. J Mater Res Bull 20:1297–1308
22. Whangbo MH, Canadell E (1988) Band electronic structure of the lithium molybdenum purple bronze $Li_{0.9}Mo_6O_{17}$. J Am Chem Soc 110:358–363
23. Collins BT, Greenblatt M, McCarroll WH, Hull GW (1988) Quasi-one-dimensionality in the new bronze-like compound $La_2Mo_2O_7$. J Solid State Chem 73:507–513
24. Wadsley AD (1967). In: Mandelcorn L (ed.) Non-stoichiometric compounds. Academic Press, New York, pp 98–209
25. Canadell E, Whangbo MH (1991) Conceptual aspects of structure-property correlations and electronic instabilities, with applications to low-dimensional transition-metal oxides. Chem Rev 91:965–1034
26. Sahle W (1983) Electron microscopy studies of tungsten oxides in the range WO_3–$WO_{2.72}$. Phase relations, defect structures, structural transformations and electrical conductivity. Chem Commun Univ Stockholm 4:1–53
27. Gebert E, Ackermann RJ (1966) Substoichiometry of tungsten trioxide; the crystal systems of $WO_{3.00}$, $WO_{2.98}$, and $WO_{2.96}$. Inorg Chem 5:136–142
28. Migas DB, Shaposhnikov VL, Rodin VN, Borisenko VE (2010) Tungsten oxides. I. Effects of oxygen vacancies and doping on electronic and optical properties of different phases of WO_3. J Appl Phys 108:093713-1–093713-7
29. Vogt T, Woodward PM, Hunter BA (1999) The high-temperature phases of WO_3. J Solid State Chem 144:209–215
30. Gerand G, Novogorocki G, Guenot J, Figlarz M (1979) Structural study of a new hexagonal form of tungsten trioxide. J Solid State Chem 29:429–434
31. Balázsi C, Farkas-Jahnke M, Kotsis I, Petrás L, Pfeifer J (2001) The observation of cubic tungsten trioxide at high-temperature dehydration of tungsten acid hydrate. Solid State Ionics 141–142:411–416
32. Szilágyi IM, Wang L, Gouma PI, Balázsi C, Madarász J, Pokol G (2009) Preparation of hexagonal WO_3 from hexagonal ammonium tungsten bronze for sensing NH_3. Mater Res Bull 44:505–508
33. Trasorras JRL, Wolfe TA, Knabl W, Venezia C, Lemus R, Lassner E, Schubert WD, Lüderitz E, Wolf HU (2016) Tungsten, tungsten alloys, and tungsten compounds. Ullmann's encyclopedia of industrial chemistry. Wiley-VCH Verlag GmbH & Co. KGaA, New York, pp 1–53
34. Schmidt P, Binnewies M, Glaum R, Schmidt M (2013) Chemical vapor transport reactions methods, materials, modeling. In: INTECH open science/open minds. https://doi.org/10.5772/55547. (Chapter 9:227–305)
35. Migas DB, Shaposhnikov VL, Rodin VN, Borisenko VE (2010) Tungsten oxides. II. The metallic nature of Magnéli phases. J Appl Phys 108:093714-1–093714-6
36. Wöhler F (1824) Ueber das Wolfram (About tungsten). Ann Physik [in German] 78:345–358
37. Dickens PG, Whittingham MS (1968) The tungsten bronzes and related compounds. Rev Chem Soc 22:30–44
38. Lunk HJ (2015) Incandescent lighting and powder metallurgical manufacturing of tungsten wire. ChemTexts 1:3. https://doi.org/10.1007/s40828-014-0003-8
39. Lunk HJ, Ziemer B, Salmen M, Heidemann D (1993–1994) What is behind 'tungsten blue oxides'? Int J Refract Metals Hard Mater 12:17–26
40. Lunk HJ, Salmen M, Heidemann D (1998) Solid-state ^{1}H-NMR studies of different tungsten blue oxides and related substances. Int J Refract Metals Hard Mater 16:23–30
41. Kim M, Park J, Kang M, Kim JY, Lee SW (2020) Toward efficient electrocatalytic oxygen evolution: emerging opportunities with metallic pyrochlore oxides for electrocatalysts and conductive supports. ACS Cent Sci 6:880–891
42. Lemoine K, Moury R, Duran E, Arroyo-de Dompablo E, Morán E, Leblanc M, Hémon-Ribaud A, Grenèche JM, Galven C, Gunes V, Lhoste J, Maisonneuve V (2021) First mixed-metal fluoride pyrochlores obtained by topotactic oxidation of ammonium fluorides under F_2 gas. Cryst Growth Des 21:935–945
43. Maričić S, Smith JAS (1958) A Nuclear magnetic resonance study of the hydrates of molybdenum trioxide. J Chem Soc 1958:886–891
44. Nakamoto K, Margoshes M, Rundle RE (1955) Stretching frequencies as a function of distances in hydrogen bonds. J Am Chem Soc 77:6480–6486. https://doi.org/10.1021/ja01629a013
45. Schröder FA, Krebs B, Mattes R (1972) Die Schwingungsspektren von $MoO_3{\cdot}2H_2O$ und $MoO_2Cl_2{\cdot}H_2O$ (Vibrational spectra of $MoO_3{\cdot}2H_2O$ and $MoO_2Cl_2{\cdot}H_2O$). Z Naturforschg [in German] 27b:22–25
46. Oswald HR, Günter JR, Dubler E (1975) Topotactic decomposition and crystal structure of white molybdenum trioxide-monohydrate: prediction of structure by topotaxy. J Solid State Chem 13:330–338
47. Krebs B (1972) Die Kristallstruktur von $MoO_3{\cdot}2H_2O$ (The crystal structure of $MoO_3{\cdot}2H_2O$). Acta Cryst [in German] B28:2222–2231. https://doi.org/10.1107/S0567740872005849
48. Schwarzmann E, Glemser O (1961) Zur Bindung des Wassers in den Hydraten des Wolframtrioxids (The bonding of water in hydrates of tungsten trioxide). Z Anorg Allg Chem [in German] 312:45–49
49. Szymański JT, Roberts AC (1984) The crystal structure of tungstite, $WO_3{\cdot}H_2O$. Canad Mineral 22:681–688
50. Günter JR, Amberg M, Schmalle H (1989) Direct synthesis and single crystal structure determination of cubic pyrochlore-type tungsten trioxide hydrate $WO_3{\cdot}0.5H_2O$. Mat Res Bull 24:289–292

51. Klinbumrung A, Thongtem T, Thongtem S (2012) Characterization of orthorhombic α-MoO_3 microplates produced by a microwave plasma process. J Nanomat. https://doi.org/10.1155/2012/930763
52. Song J, Ni X, Gao L, Zheng H (2007) Synthesis of metastable h-MoO_3 by simple chemical precipitation. Mat Chem Phys 102:245–248
53. Vargas-Consuelos CI, Camacho-López M (2014) A facile method to prepare hexagonal molybdenum trioxide microrods. Superficies y Vacio 27:123–125
54. Song J, Ni X, Song J, Ni X, Zhang D, Zheng H (2006) Fabrication and photoluminescence properties of hexagonal MoO_3 rods. Solid State Sci 8:1164–1167
55. Tran TA, Krishnamoorthy K, Song YW, Cho SK, Kim SJ (2014) Toxicity of nano molybdenum trioxide toward invasive breast cancer cells. ACS Appl Mater Interf 6:2980–2986
56. Kraft A (2019) Electrochromism: a fascinating branch of electrochemistry. ChemTexts 5:1. https://doi.org/10.1007/s40828-018-0076-x
57. Wu CM, Naseem S, Chou MH, Wang JH, Jian YQ (2019) Recent advances in tungsten-oxide-based materials and their applications. https://doi.org/10.3389/fmats.2019.00049
58. Guggenbichler JP (2022) Dramatic increase of multi-resistant microorganisms is self-inflicted. Effective and easy solutions are available. J Clin Med Images 6:1–5
59. Vincent JL, Rello J, Marshall J, Silva E, Anzueto A, Martin CD, Moreno R, Lipman J, Gomersall C, Sakr Y, Reinhart K, for the EPOC II Group of Investigators (2009) International study of the prevalence and outcomes of infection in intensive care units. JAMA 302:2323–2329
60. National Nosocomial Infections Surveillance (NNIS) Report, data summary from January 1992 to June 2002 issued August 2002. Am J Infect Contr 30:458–475
61. Hutchings MI, Truman AW, Wilkinson B (2019) Antibiotics: past, present and future. Curr Opin Microbiol 51:72–80
62. https://www.n-tv.de/wissen/Antibiotika-Resistenz-fordert-1.2-Millionen-Opfer-article23069318.html
63. Brook I (2013) Acute sinusitis in children. Pediatr Clin North Am 60:409–424
64. Magalhães C, Lima M, Trieu-Cuot P, Ferreira P (2021) To give or not to give antibiotics is not the only question. Lancet Infect Dis 21:e191–e201
65. Han D, Wang N, Zhang L (2009) The effect of myrtol standardized on human nasal ciliary beat frequency and mucociliary transport time. Am J Rhinol Allergy 23:610–614
66. Lunk HJ, Hartl H (2021) The fascinating polyoxometalates. ChemTexts 7:26. https://doi.org/10.1007/s40828-021-00145-y
67. Zollfrank C, Gutbrod K, Wechsler P, Guggenbichler JP (2012) Antimicrobial activity of transition metal acid MoO_3 prevents microbial growth on material surfaces. Mat Sci Eng C 32:47–54
68. Guggenbichler JP, Lunk HJ (Anmeldetag 26.04.2013) Verfahren zum Herstellen eines dotierten oder undotierten Mischoxids für einen Verbundwerkstoff und Verbundwerkstoff mit einem solchen Mischoxid Anmeldung Nr./Patent Nr. 14723744.0–1354; Priorität: DE/26.04.13/DEA102013104284; Aktenzeichen 10 2013 104 284.8, IPC Hauptklasse C01G 41/02 (Method for producing a doped or undoped mixed oxide for a composite material, and a composite material comprising such a mixed oxide, pending US patent application, publication number: 20160106108, Filed: April 25, 2014; Publication date: April 21, 2016; Applicant: AMISTEC GMBH & CO. KG, Inventors: Hans-Joachim Lunk, Joseph-Peter Guggenbichler
69. Salje A, Gehlig R, Viswanathan K (1978) Structural phase transition in mixed crystals $W_xMo_{1-x}O_3$. J Solid State Chem 25:239–250
70. Cheetham AK (1980) Low-temperature preparation of refractory alloys. Nature 288:469–470
71. Morandi S, Paganini MC, Giamello E, Bini M, Capsoni D, Massarotti V, Ghiotti G (2009) Structural and spectroscopic characterization of $Mo_{1-x}W_xO_{3-\delta}$ mixed oxides. J Solid State Chem 182:3342–3352
72. Hibble SJ, Dickens PG (1985) Hydrogen insertion compounds of the mixed molybdenum tungsten oxides $Mo_yW_{1-y}O_3$ ($0.1<y<0.9$). Mat Res Bull 20:343–349
73. Ganapathi L, Ramanan A, Gopalakrishnan J, Rao CNR (1986) A study of MoO_3, WO_3, and their solid solutions prepared by topotactic dehydration of the monohydrates. J Chem Soc Chem Commun 1986:62–63
74. Figlarz M (1989) New oxides in the WO_3–MoO_3 system. Prog Solid State Chem 19:1–46
75. Garcia PF, McCarron EM (1988) Metal oxides of molybdenum or molybdenum and tungsten. U.S. Patent 4,753,916
76. McCarron III EM, Parise JB (1991) Process for preparation of metal oxides of molybdenum or molybdenum and tungsten. U.S. Patent 5,055,441